Role of dipolar interaction in magnetic hyperthermia

Gabriel T. Landi*
Instituto de Física da Universidade de São Paulo, 05314-970 São Paulo, Brazil
(Received 18 June 2013; revised manuscript received 1 November 2013; published 6 January 2014)

The dynamic properties of magnetic nanoparticles are known to be substantially influenced by the dipole-dipole interaction. In this paper we study how this affects the efficiency of magnetic hyperthermia experiments. In particular we ask whether it is possible to use the dipolar interaction as a mechanism to increase the heat released by the nanoparticles, thus improving the application. The investigation is carried out via numerical simulations based on a mean-field model developed to include the dipolar interaction in the Fokker-Planck equation describing the time evolution of the system. Both the linear and nonlinear regimes (related to the amplitude of the external magnetic field) are studied in detail. It is shown that even moderate changes in the particle concentration may have substantial effects on the magnetization dynamics of the system, being capable of increasing or decreasing the heat released by orders of magnitude, depending on the values of other system parameters. It is found that the dipolar interaction can be used to increase the dissipation of magnetically soft particles, but should be avoided in the case of hard particles.

DOI: 10.1103/PhysRevB.89.014403 PACS number(s): 75.60.−d, 75.75.Jn, 05.10.Gg

I. INTRODUCTION

The physics of small magnetic particles is extremely rich and has been studied in great detail over the past decades. Most notably, these materials present a phenomenon known as superparamagnetism,[1,2] whereby each particle behaves as a classical paramagnet (albeit with an enormous magnetic moment). Another peculiarity is the strong dependence on the thermal fluctuations. This is understood by noting that each particle is also influenced by local anisotropy potentials, which are usually bistable in nature, the barrier separating the energy minima being roughly proportional to Kv, where K is the anisotropy constant and v is the volume. It thus follows that, due to their reduced dimensions, the ratio $\sigma = Kv/kT$ may be of the order of unity, meaning that the thermal fluctuations are capable of exciting frequent transitions between the energy minima. Hence, small magnetic particles are characterized by an intricate competition between the external magnetic field, the internal anisotropy potential, and the thermal fluctuations.

A variety of applications have been proposed which, directly or indirectly, exploit this interdependence. One, which has advanced substantially in recent years, is magnetic hyperthermia.[3–6] It uses the heat released by the particles under the influence of a high-frequency magnetic field, $H = H_0 \cos \omega t$, to locally heat up (and thus kill) cancer cells. The efficacy of this application is usually measured using the specific absorption rate (SAR), which is the power released by the particles in the form of heat. One may argue[7] that a promising route to maximize the SAR is precisely by exploiting the aforementioned interdependence with temperature. As an example, note that for small-field amplitudes we have from the linear response theory that

$$\mathrm{SAR} \sim \frac{\omega\tau}{1+(\omega\tau)^2},$$

where $\tau \sim e^{\sigma}$ is the relaxation time. Hence, to optimize the experiment one should attempt to set the frequency to satisfy $\omega\tau \sim 1$. Microscopically, this is interpreted as follows. Most of the heat dissipated stems from irreversible jumps of the magnetization between the barrier separating the energy minima. Hence, maximizing the SAR is tantamount to maximizing the number of such jumps. The height of the barrier, however, is also relevant. For low σ the barrier is shallow and the jumps occur frequently, irrespective of the smallness of the field amplitude. The energy released in each jump, however, is small. Conversely, for large σ the number of jumps is small but the energy released in each one is large. The condition $\omega\tau \sim 1$ is thus seen as the optimum point between both regimes and determines the value σ_{opt} which maximizes the SAR. In conclusion, by adjusting the external field's parameters with intrinsic properties of the particles and the environment, it is possible to increase the efficiency of the experiment by orders of magnitude.

There is another property present in most systems which, to my knowledge, has never been exploited in the above sense, namely the dipole-dipole interaction between the particles. The practical relevance of this effect has been demonstrated by several experiments[8–14] and numerical simulations.[15–22] By itself, it is already of fundamental importance; for instance, the exact way with which it affects the dynamics of the system is still an open question.[23] In addition, however, and in view of the arguments just given, it is reasonable to ask whether the dipolar interaction may also be exploited to optimize the SAR. It is the purpose of this paper to give a partial answer to this question. This will be accomplished by numerical simulations of the SAR using a mean-field model developed in Ref. 24. This approach, as will be shown, is computationally very efficient, thus having the advantage of allowing an ample investigation of the influence of all important parameters. This is, in my view, of substantial scientific relevance given that both experimental and simulation (e.g., Monte Carlo) studies are always limited by a finite number of samples.

II. MEAN-FIELD MODEL

Recently, I have worked out a mean-field model for the dipolar interaction[24] which predicts an increase in the effective magnetic anisotropy barrier.[25] Let $\sigma = Kv/kT$ be again this barrier in an infinitely diluted system. Then, the modified

barrier according to this model is

$$\sigma_{\rm eff} = \sigma + \gamma\sigma^2 p_2, \tag{1}$$

where p_2 is the average of a Legendre polynomial ($p_2 \sim 0.9$) and

$$\gamma = \frac{N}{10}\left(\frac{\langle\mu^2\rangle\mu_0}{4\pi K v}\right)^2\left\langle\frac{1}{R^6}\right\rangle. \tag{2}$$

Here N is the total number of particles in the system, μ_0 is the permeability of vacuum, μ is the magnetic moment, and R is the interparticle distance; $\langle\mu^2\rangle$ and $\langle 1/R^6\rangle$ are the statistical averages of these quantities. This result show an extremely strong dependence of $\sigma_{\rm eff}$ on the interparticle distance: slight increases in the concentration may lead to substantial increases in the anisotropy barrier. This is even more salient in the high-barrier regime ($\sigma \gg 1$) due to the quadratic dependence in the last term of Eq. (1). It is worth noting that one of the premises of this model is that the particles are assumed to be randomly distributed in space and, in the process of constructing the mean-field approximation, the actual form of the sample does not enter (this is clearly an artificiality in the model since the shape of the sample is known to be important).

In this paper I propose to use this model to investigate the role of the dipolar interaction in the dynamic properties of magnetic nanoparticles, and how this affects the SAR in hyperthermia experiments. This will be accomplished numerically, by introducing a modified effective potential in the Fokker-Planck equation that describes the stochastic time evolution of the system. It will be shown that both in the linear and the nonlinear regimes, the dipolar interaction may have a profound influence on the SAR and other properties, even for quite diluted systems. By tuning the particle concentration, it will be shown that the SAR can be enhanced by up to two orders of magnitude. Conversely, in other situations it may be hindered by similar, if not worse, amounts.

The calculations will assume that the external magnetic field is collinear with the anisotropy easy axis. As has been shown,[26] this approximation is entirely reasonable, at least with regards to the qualitative behavior of the system. The variable of interest is thus $z = \cos\theta$, the angle that the magnetization vector makes with the easy axis. The effective free energy, as developed in Ref. 24, is given by

$$-\frac{\mathcal{U}_{\rm eff}}{k_B T} = 2\sigma h z + (\sigma + \gamma\sigma^2 p_2)z^2, \tag{3}$$

where $p_\ell = \langle P_\ell(z)\rangle$ is the expectation of a Legendre polynomial of degree ℓ in z (the fact that the free energy depends on the expectation of z, and not only on z itself, is due to the mean-field nature of the model).

Equation (3) is actually the first term in an expansion in the parameter γ, which measures the strength of the dipolar interaction. We are therefore assuming explicitly that the interaction is weak in order to truncate at first order. Based on estimates made in Ref. 26 (see also Sec. IV), this is a reasonable approximation. One of the main results of the model developed in Ref. 26 is that the first correction is proportional to z^2 and hence acts to increase the effective anisotropy barrier. Consequently, this correction does not predict any phase transitions. The second order correction, however, contains a term proportional to z^3 *and* a term proportional to z. The latter, as was shown in Ref. 26, does induce a phase transition to a ferromagnetic state. Hence, in the present analysis we are ignoring higher order corrections that can induce phase transitions and working within first order in the intensity of the dipolar interaction.

The field $h = h_0\cos\omega t$ is given in reduced units: $h = \mu H/(2Kv)$. The effective field stemming from the free energy (3) is

$$h_{\rm eff} = -\frac{1}{k_B T}\frac{\partial\mathcal{U}_{\rm eff}}{\partial z} = 2\sigma h + 2(\sigma + \gamma\sigma^2 p_2)z. \tag{4}$$

This field enters in the Fokker-Planck equation for the time evolution of $f(z,t)$, the probability density of z; viz.,[24,26–29]

$$2\tau_N\frac{\partial f}{\partial t} = \frac{\partial}{\partial z}\left\{(1-z^2)\left[\frac{\partial f}{\partial z} - f(z,t)h_e(z,t)\right]\right\}, \tag{5}$$

where $\tau_N = \mu(1+\alpha^2)/(2\gamma_0\alpha k_B T)$ is the Néel relaxation time (α is the magnetization damping and γ_0 is the electron's gyromagnetic ratio).

The Fokker-Planck equation may be used to obtain an equation for the time evolution of $p_\ell = \langle P_\ell(z)\rangle$. As shown in Ref. 24, this is given by

$$2\tau_N\frac{dp_\ell}{dt} = \frac{\ell(\ell+1)}{2\ell+1}(\mathcal{A}_1 + \mathcal{A}_2) - \ell(\ell+1)p_\ell, \tag{6}$$

where

$$\mathcal{A}_1 = 2\sigma h(p_{\ell-1} - p_{\ell+1}),$$

$$\mathcal{A}_2 = 2(\sigma + \gamma\sigma^2 p_2)\left[\frac{\ell-1}{2\ell-1}p_{\ell-2} + \frac{2\ell+1}{(2\ell-1)(2\ell+3)}p_\ell - \frac{\ell+2}{2\ell+3}p_{\ell+2}\right].$$

This constitutes an infinite hierarchy of differential-recurrence relations for the p_ℓ. Unlike in the infinitely diluted case ($\gamma = 0$), this system is nonlinear due to the product with p_2 appearing in $\mathcal{A}_2$. Organizing the equations we may write, using the sum convention,

$$\frac{dp_i}{dt} = a_i + a_{ij}p_j + a_{ijk}p_j p_k.$$

The last term is zero when $\gamma = 0$, thus recovering the linear hierarchy of the infinitely diluted case. Alternatively we may define $\boldsymbol{p} = (p_1, p_2, \ldots, p_n)$, where n is some large enough truncation value; then

$$\frac{d\boldsymbol{p}}{dt} = \boldsymbol{F}(\boldsymbol{p}),$$

where $\boldsymbol{F}$ is a vector-valued function of $\boldsymbol{p}$. This system of ordinary differential equations is solved numerically[26] for a large enough value of n (to ensure convergence). After discarding several periods of the external field, we obtain a steady-state hysteresis loop (the variable of interest is $p_1 = \langle z\rangle$). The SAR is computed from the area A of this loop by numerical quadrature: SAR $= (\omega/2\pi)A$. The free parameters are σ, γ, h_0, and ω but, for simplicity,[30] we fix $\omega\tau_N = 10^{-4}$.

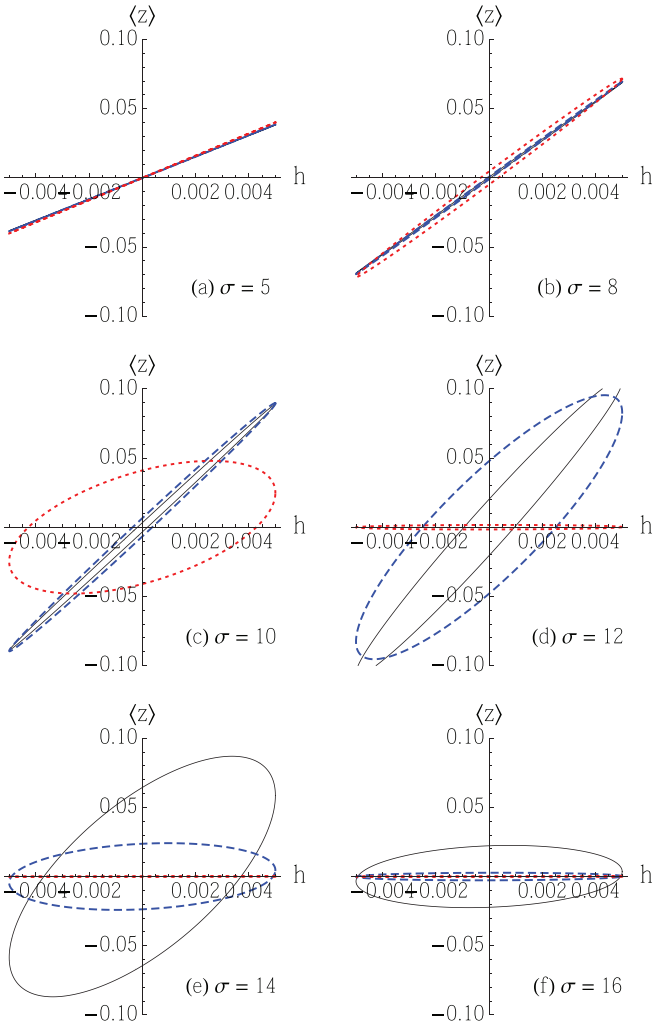

FIG. 1. (Color online) Hysteresis loops in the linear regime, $h_0 = 0.005$. From (a) to (f), different values of σ, as denoted. Black solid, $\gamma = 0$; blue dashed, $\gamma = 0.01$; red dotted, $\gamma = 0.05$.

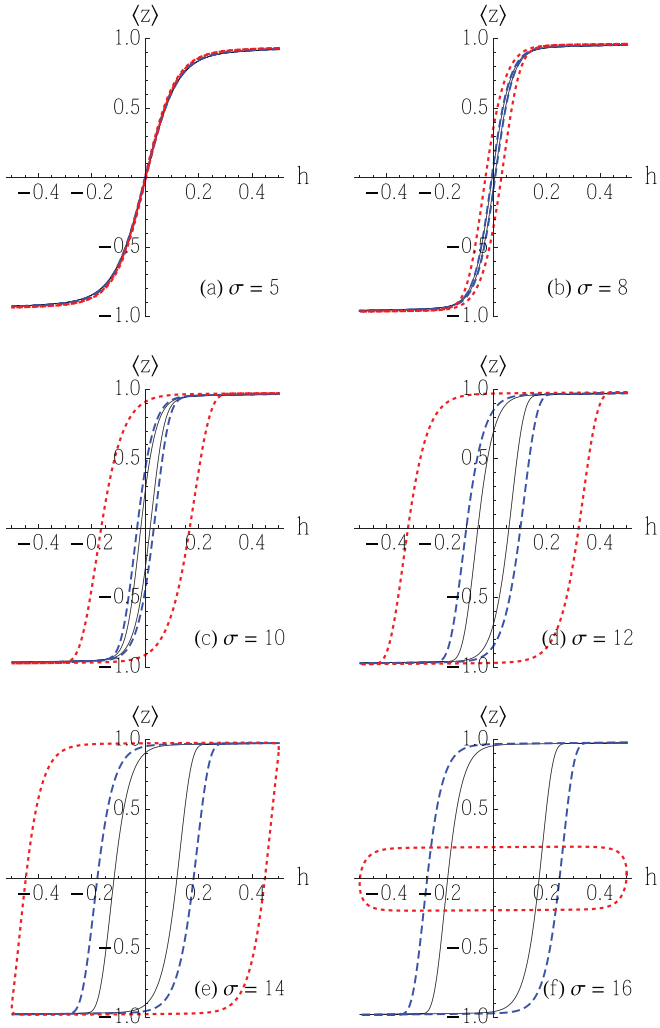

FIG. 2. (Color online) Hysteresis loops in the nonlinear regime, $h_0 = 0.5$. All other details are similar to Fig. 1.

III. NUMERICAL RESULTS

In Figs. 1 and 2 we present hysteresis loops for the linear ($h_0 = 0.005$) and nonlinear ($h_0 = 0.5$) regimes, respectively. In each figure we show curves for $\gamma = 0$, 0.01, and 0.05. It is very important to highlight that, for instance, a fivefold increase in γ means, according to Eq. (2), a mere 30% decrease in the interparticle distance. Let us start with the infinitely diluted case (black solid curves). For low values of σ we first observe the "high temperature" regime where the loops resemble paramagnetic systems, with a small area. Then, upon increasing σ, we see that the area of the loops reach a maximum (when $\sigma = 14$) which then falls for even larger σ. This is a manifestation of the effect discussed in the beginning of the paper about the maximum occurring at $\omega\tau \sim 1$.

Next we turn to the case $\gamma \neq 0$. The main point to be seen in Fig. 1 is that the dipolar interaction may both increase and decrease the hysteresis loop area, depending on the value of σ. Up to $\sigma = 10$ one observes an increase in the area upon increasing γ, which is modest at first but pronounced for $\sigma = 10$. Conversely, when $\sigma \geqslant 12$ it is possible to see first an increase when $\gamma = 0.01$ (blue dashed curves) followed by a substantial drop when $\gamma = 0.05$ (red dotted curves).

In the nonlinear regime (Fig. 2) a similar behavior is observed. The curves now tend to behave more like bulk hysteresis loops. When $\gamma = 0$, the area continues to increase all the way up to $\sigma = 16$. By introducing the dipolar interaction, however, this changes dramatically. Now up to $\sigma = 14$, increasing γ enhances the area substantially. Then, for $\sigma = 16$, an abrupt diminution of the loop height is observed. These results indicate, as mentioned in the beginning of the paper, that the effect of the dipolar interaction can be extremely strong leading to abrupt variations even for small changes in the parameters.

The dependence of the SAR with the anisotropy barrier σ is shown in Fig. 3 for both the linear and nonlinear regimes. Starting once again with the linear regime, the SAR is seen to present an accentuated peak. As γ increases this peak is shifted to the left and narrowed further, its maximum height also diminishing. The behavior in the nonlinear regime is

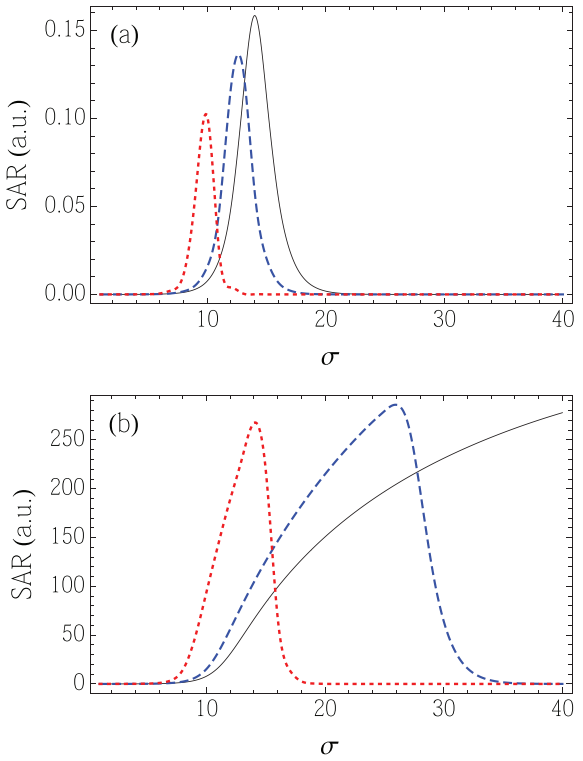

FIG. 3. (Color online) The SAR as a function of σ for different values of γ in the linear regime [$h_0 = 0.005$; panel (a)] and nonlinear regime [$h_0 = 0.5$; panel (b)]. Black solid, $\gamma = 0$; blue dashed, $\gamma = 0.01$; red dotted, $\gamma = 0.05$.

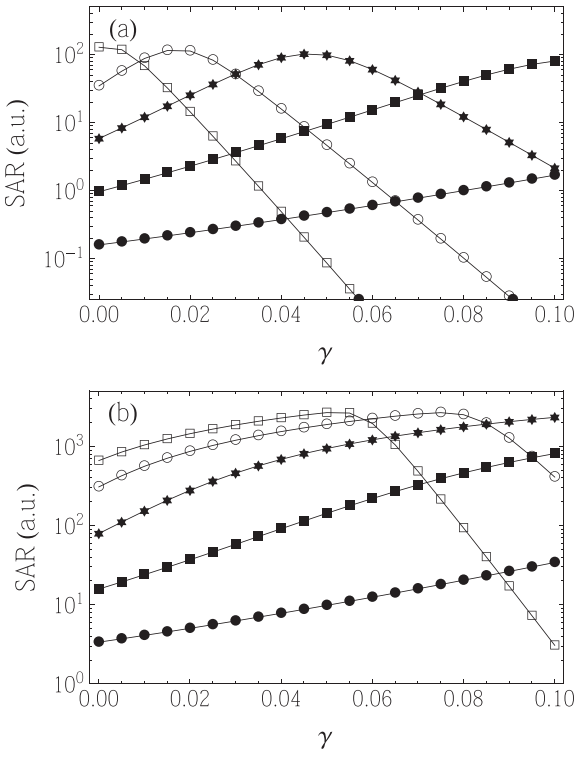

FIG. 4. The SAR as a function of γ for different values of σ in the linear [$h_0 = 0.005$; panel (a)] and nonlinear regime [$h_0 = 0.5$; panel (b)]. Filled circles, $\sigma = 6$; filled squares, $\sigma = 8$; stars, $\sigma = 10$; open circles, $\sigma = 12$; open squares, $\sigma = 14$.

entirely different. When $\gamma = 0$ there is no peak, but rather a broad curve that extends well into much higher values of σ. Profound changes are then observed due to the dipolar interaction. The curve now gradually approaches a more finely peaked behavior and is substantially shifted to smaller values of σ.

Finally, in Fig. 4 we present the SAR as a function of γ. Upon noticing the logarithmic scale in the ordinate, it is possible to fathom the remarkable effect that γ (i.e., the dipolar interaction) has in the SAR. It may, for some values of σ, increase the SAR by up to two orders of magnitude while, for other values, decrease it by more than four orders of magnitude. Let us highlight some of the more interesting behaviors. We start with the curve for $\sigma = 10$ in Fig. 4(a) (stars). It first increases by a factor of 10 and then decreases as γ is increased further. Another remarkable example is the curve for $\sigma = 14$ in the nonlinear regime [Fig. 4(b), open squares]. It increases gradually up to $\gamma = 0.06$ and then abruptly falls by almost 3 orders of magnitude as γ goes from 0.06 to 0.1. This corresponds to a mere 10% further increase in the concentration. Finally, it is interesting to note the behavior of the soft particles, $\sigma = 6$ [Figs. 4(a) and 4(b), filled circles]. It shows a gradual increase in the SAR with increasing γ. Thus, whereas for $\gamma = 0$ this condition would not be suitable for hyperthermia due to its low SAR, upon introducing the dipolar interaction it becomes comparable with other conditions and thus appropriate for the application.

IV. DISCUSSION AND CONCLUSIONS

From the analysis of the previous result we conclude that the ranges of σ in which the SAR increases or decreases is roughly related to the position σ_{opt} that maximizes $\omega\tau \sim 1$. This is the peak of the black solid curve in Fig. 3(a). Since, upon increasing γ, we observe a shift to the left, we expect an increase in the SAR upon increasing γ when $\sigma < \sigma_{\text{opt}}$, with the converse being expected in the complementary interval. The reason is as follows. When $\sigma < \sigma_{\text{opt}}$ we are in the low-barrier regime where the jumps are frequent but the energy released in each jump is small. Increasing the dipolar interaction increases the anisotropy barrier and thus takes the system closer to the optimum condition $\sigma_{\text{opt}} \sim \omega\tau$. Conversely, when $\sigma > \sigma_{\text{opt}}$ we are in the high-barrier regime where the external field already has a substantial difficulty in promoting the jumps. Thus, increasing the dipolar interaction merely increases the height even more, further hampering the efficacy of the process. This analysis is only approximate but does provide useful physical insight. It is, however, more fitting of the linear regime where the external field is unable to bend the anisotropy potential. The nonlinearity introduced by this bending makes the analysis more difficult but it may be conjecture that, notwithstanding, the main conclusions remain roughly true.

It is certainly expected that effects such as the size distribution should play a role in analyzing these results. However, experience shows that their influence is more in the effect of smoothing some of the more abrupt features

of monodisperse systems, rather than completely destroying them.

Let us briefly compare our results with the literature on interacting magnetic nanoparticles. In Ref. 16 the dipolar interaction is investigated via simulations of the stochastic Landau-Lifshitz equation. The authors found a decrease in the SAR with particle concentration. However, by analyzing their parameters we see that their simulations are for the regime where $\omega\tau \gg 1$; this is the blocked regime where $\sigma \gg \sigma_{\text{opt}}$. Their results are therefore in complete agreement with ours. See, for instance, the curve with $\sigma = 14$ in Fig. 4. In Ref. 15, Mehdaoui *et al*. observe, both experimentally and theoretically, an increase in the hyperthermia efficiency due to the dipolar interactions when the magnetic particles are soft. This correspond to $\omega\tau \ll 1$, which again agrees with our results (cf. the curve for $\sigma = 6$ in Fig. 4). Finally, it is worth commenting that Martinez-Boubeta *et al*.,[14] who experimentally studied interacting core-shell particles, reached the same qualitative conclusions about the dipolar interaction, namely that for soft particles, upon increasing the concentration, the SAR first increases up to a point where the dipolar interaction becomes comparable with the anisotropy field, after which it starts to decrease with concentration.

To finish, let us make a rough estimate of γ, Eq. (2). We may take $\mu \sim 10^4 \mu_B$, $R \sim 30$ nm, $Kv \sim 5k_BT$, $T = 300$ K, and $N \sim 10^5$. This yields $\gamma \sim 0.02$, well within the bounds studied in this paper.

In conclusion we have analyzed the role of the dipolar interaction in the specific absorption rate (heat released by the particles) in the context of magnetic hyperthermia. The analysis was performed using a mean-field model derived in Ref. 24. It predicts a strong influence of the dipolar interaction on the SAR, being capable of both increasing and decreasing it, depending on the other system parameters, σ, h_0, and ω. The main result of this paper is that magnetically soft particles, which usually have a low SAR, can profit from the dipolar interaction which increases the energy barrier and thus improves the SAR. On the other hand, magnetically hard particles are seen to be further hampered by increasing the dipolar interaction due to a larger freezing of the magnetic spins. These results follow directly from the fact that the dipolar interaction acts to increase the effective anisotropy barrier. Their strength, however, could only be realized by the numerical simulations performed and, as was observed, can be extremely strong depending on the other system parameters. It is hoped that, exploiting these results, one may use the dipolar interaction beneficially, as a mechanism to increase the SAR in hyperthermia experiments.

ACKNOWLEDGMENT

The author would like to acknowledge the Brazilian funding agency FAPESP for financial support.

*gtlandi@gmail.com

[1] L. Néel, Ann. Géophys **5**, 99 (1949).
[2] C. Bean and I. Jacobs, J. Appl. Phys. **27**, 1448 (1956).
[3] R. K. Gilchrist, R. Medal, W. D. Shorey, R. C. Hanselman, J. C. Parrott, and C. B. Taylor, Annals of Surgery **146**, 596 (1957).
[4] J. Carrey, B. Mehdaoui, and M. Respaud, J. Appl. Phys. **109**, 083921 (2011).
[5] Q. A. Pankhurst, N. K. T. Thanh, S. K. Jones, and J. Dobson, J. Phys. D **42**, 224001 (2009).
[6] E. L. Verde, G. T. Landi, J. A. Gomes, M. H. Sousa, and A. F. Bakuzis, J. Appl. Phys. **111**, 123902 (2012); E. L. Verde, G. T. Landi, M. S. Carrião, A. L. Drummond, J. A. Gomes, E. D. Vieira, M. H. Sousa, and A. F. Bakuzis, AIP Advances **2**, 032120 (2012).
[7] G. T. Landi and A. F. Bakuzis, J. Appl. Phys. **111**, 083915 (2012).
[8] J. L. Dormann, F. D'Orazio, F. Lucari, E. Tronc, P. Prené, J. P. Jolivet, D. Fiorani, R. Cherkaoui, and M. Noguès, Phys. Rev. B **53**, 14291 (1996).
[9] T. Jonsson, J. Mattsson, C. Djurberg, F. A. Khan, P. Nordblad, and P. Svedlindh, Phys. Rev. Lett. **75**, 4138 (1995); T. Jonsson, J. Mattsson, P. Nordblad, and P. Svedlindh, J. Magn. Magn. Mater. **168**, 269 (1997).
[10] S. H. Masunaga, R. F. Jardim, R. S. Freitas, and J. Rivas, Appl. Phys. Lett. **98**, 013110 (2011); S. H. Masunaga, R. F. Jardim, P. F. P. Fichtner, and J. Rivas, Phys. Rev. B **80**, 184428 (2009); S. H. Masunaga, R. F. Jardim, and J. Rivas, J. Appl. Phys. **109**, 07B521 (2011).
[11] J. Sung Lee, R. P. Tan, J. H. Wu, and Y. K. Kim, Appl. Phys. Lett. **99**, 062506 (2011).
[12] C. L. Dennis, A. J. Jackson, J. A. Borchers, R. Ivkov, A. R. Foreman, J. W. Lau, E. Goernitz, and C. Gruettner, J. Appl. Phys. **103**, 07A319 (2008).
[13] A. Urtizberea, E. Natividad, A. Arizaga, M. Castro, and A. Mediano, J. Phys. Chem. C **114**, 4916 (2010).
[14] C. Martinez-Boubeta, K. Simeonidis, D. Serantes, I. Conde-Leborán, I. Kazakis, G. Stefanou, L. Peña, R. Galceran, L. Balcells, C. Monty, D. Baldomir, M. Mitrakas, and M. Angelakeris, Adv. Funct. Mater. **22**, 3737 (2012).
[15] B. Mehdaoui, R. P. Tan, A. Meffre, J. Carrey, S. Lachaize, B. Chaudret, and M. Respaud, Phys. Rev. B **87**, 174419 (2013).
[16] C. Haase and U. Nowak, Phys. Rev. B **85**, 045435 (2012).
[17] C. Verdes, B. Ruiz-Diaz, S. M. Thompson, R. W. Chantrell, and A. Stancu, Phys. Rev. B **65**, 174417 (2002).
[18] D. Serantes, D. Baldomir, C. Martinez-Boubeta, K. Simeonidis, M. Angelakeris, E. Natividad, M. Castro, A. Mediano, D.-X. Chen, A. Sanchez, L. Balcells, and B. Martinez, J. Appl. Phys. **108**, 073918 (2010).
[19] D. Kechrakos and K. N. Trohidou, Appl. Phys. Lett. **81**, 4574 (2002).
[20] D. Kechrakos and K. N. Trohidou, Phys. Rev. B **58**, 12169 (1998).
[21] J. Dormann, D. Fiorani, and E. Tronc, J. Magn. Magn. Mater. **202**, 251 (1999).
[22] J.-O. Andersson, C. Djurberg, T. Jonsson, P. Svedlindh, and P. Nordblad, Phys. Rev. B **56**, 13983 (1997).
[23] P.-M. Dejardin, J. Appl. Phys. **110**, 113921 (2011).
[24] G. T. Landi, J. Appl. Phys. **113**, 163908 (2013).
[25] This idea traces back to the works of Wolfarth and collaborators (Ref. 31).
[26] G. T. Landi, J. Appl. Phys. **111**, 043901 (2012).
[27] W. F. Brown, Phys. Rev. **130**, 1677 (1963).

[28]W. T. Coffey, Y. P. Kalmykov, and J. T. Waldron, *The Langevin Equation, with Applications to Stochastic Problems in Physics, Chemistry, and Electrical Engineering*, 2nd ed. (World Scientific Publishing Co., Pte. Ltd., Singapore, 2004), p. 678.

[29]G. T. Landi and A. D. Santos, J. Appl. Phys. **111**, 07D121 (2012).

[30]This is not restrictive. The condition $\omega\tau \sim 1$ implies $\sigma_{\rm opt} \sim \log\omega\tau_N$. Hence, changing the frequency produces, at most, *logarithmic* changes.

[31]R. W. Chantrell and E. P. Wohlfarth, J. Magn. Magn. Mater. **40**, 1 (1983); S. Shtrikman and E. P. Wohlfarth, Phys. Lett. A **85**, 467 (1981).